Journal of Volcanology and Geothermal Research 180 (2009) 135–147

Contents lists available at ScienceDirect

Journal of Volcanology and Geothermal Research

journal homepage: www.elsevier.com/locate/jvolgeores

Observations of Mt. Etna volcanic ash plumes in 2006: An integrated approach from ground-based and polar satellite NOAA–AVHRR monitoring system

D. Andronico [a,*], C. Spinetti [b], A. Cristaldi [a], M.F. Buongiorno [b]

[a] Istituto Nazionale di Geofisica e Vulcanologia, Sezione di Catania, Italy
[b] Istituto Nazionale di Geofisica e Vulcanologia, Sezione CNT, Roma, Italy

ARTICLE INFO

Available online 24 November 2008

Keywords:
volcanic ash
Mt. Etna
ground monitoring
NOAA–AVHRR

ABSTRACT

Mt. Etna, in Sicily (Italy), is one of the world's most frequent emitters of volcanic plumes. During the last ten years, Etna has produced copious tephra emission and fallout that have damaged the inhabited and cultivated areas on its slopes and created serious hazards to air traffic. Recurrent closures of the Catania International airport have often been necessary, causing great losses to the local economy. Recently, frequent episodes of ash emission, lasting from a few hours to days, occurred from July to December 2006, necessitating a look at additional monitoring techniques, such as remote sensing. The combination of a ground monitoring system with polar satellite data represents a novel approach to monitor Etna's eruptive activity, and makes Etna one of the few volcanoes for which this surveillance combination is routinely available.

In this work, ash emission information derived from an integrated approach, based on comparing ground and NOAA–AVHRR polar satellite observations, is presented. This approach permits us to define the utility of real time satellite monitoring systems for both sporadic and continuous ash emissions. Using field data (visible observations, collection of tephra samples and accounts by local inhabitants), the duration and intensity of most of the tephra fallout events were evaluated in detail and, in some cases, the order of magnitude of the erupted volume was estimated. The ground data vs. satellite data comparison allowed us to define five different categories of Etna volcanic plumes according to their dimensions and plume height, taking into account wind intensity. Using frequent and good quality satellite data in real time, this classification scheme could prove helpful for investigations into a possible correlation between eruptive intensity and the presence and concentration of ash in the volcanic plume. The development and improvement of this approach may constitute a powerful warning system for Civil Protection, thus preventing unnecessary airport closures.

1. Introduction

Volcanic plumes are mixtures of solid particles and gases in different proportions that rise up above active volcanoes. Gases are exsolved from magma and water or incorporated from the atmosphere during eruptions (Sparks et al., 1997). Therefore, plumes are a visible indicator of eruptive activity.

In recent years, the detection of ash-enriched plumes has become an important goal for volcanologists and civil institutions. Due to increasing air traffic, volcanic plumes constitute a primary source of hazard for aviation all over the world (Casadevall, 1994; Miller and Casadevall, 2000). There is no definition of a safe level of ash exposure for aircraft, and the "standard" atmosphere is normally considered to be free from volcanic ash (ICAO, 2004; FAA, 2001).

To mitigate and prevent this high risk is thus crucial, and a number of investigations have been performed to detect volcanic plumes in the most hazardous areas, particularly in cloudy or night time conditions. New sophisticated instrumentations have been studied and tested in proximity of active volcanoes, using several technologies to detect ash plumes (e.g. Andò and Pecora, 2006; Francis and Rothery, 2000).

One of the biggest producers of volcanic plumes in the world is Mt. Etna volcano in Sicily, Italy (Fig. 1). Such plumes are clearly visible both in quiet degassing periods as well as during eruptions (Allard et al., 1991; Haulet et al., 1977). Due to this quasi-persistent eruptive activity, there is a constant and serious hazard to both international and local air traffic, particularly if the eruption is highly explosive. The formation of volcanic plumes from Etna may occur both from the summit craters (located between 3000 and 3300 m a.s.l.; Fig. 1) and from eruptive fractures that often open on the flanks of the volcano. In recent years, Etna has frequently shown powerful explosive activity, including episodic paroxysms (more than 150 events since 1995; Alparone et al., 2007) and long-lasting explosive eruptions such as during 2001 for about 20 days (INGV-Staff, 2001; Scollo et al., 2007) and in 2002–03 for about 2 months (Andronico et al., 2003, 2005, 2008). Etna also undergoes intense degassing during periods of apparent quiescence or no eruptive activity. Continuous production of gas-enriched plumes is caused by the ordinary degassing occurring at its summit. This kind of

* Corresponding author. Piazza Roma 2, 95123 Catania, Italy. Tel.: +39 095 7165800; fax: +39 095 435801.
E-mail address: andronico@ct.ingv.it (D. Andronico).

0377-0273/$ – see front matter © 2008 Elsevier B.V. All rights reserved.
doi:10.1016/j.jvolgeores.2008.11.013

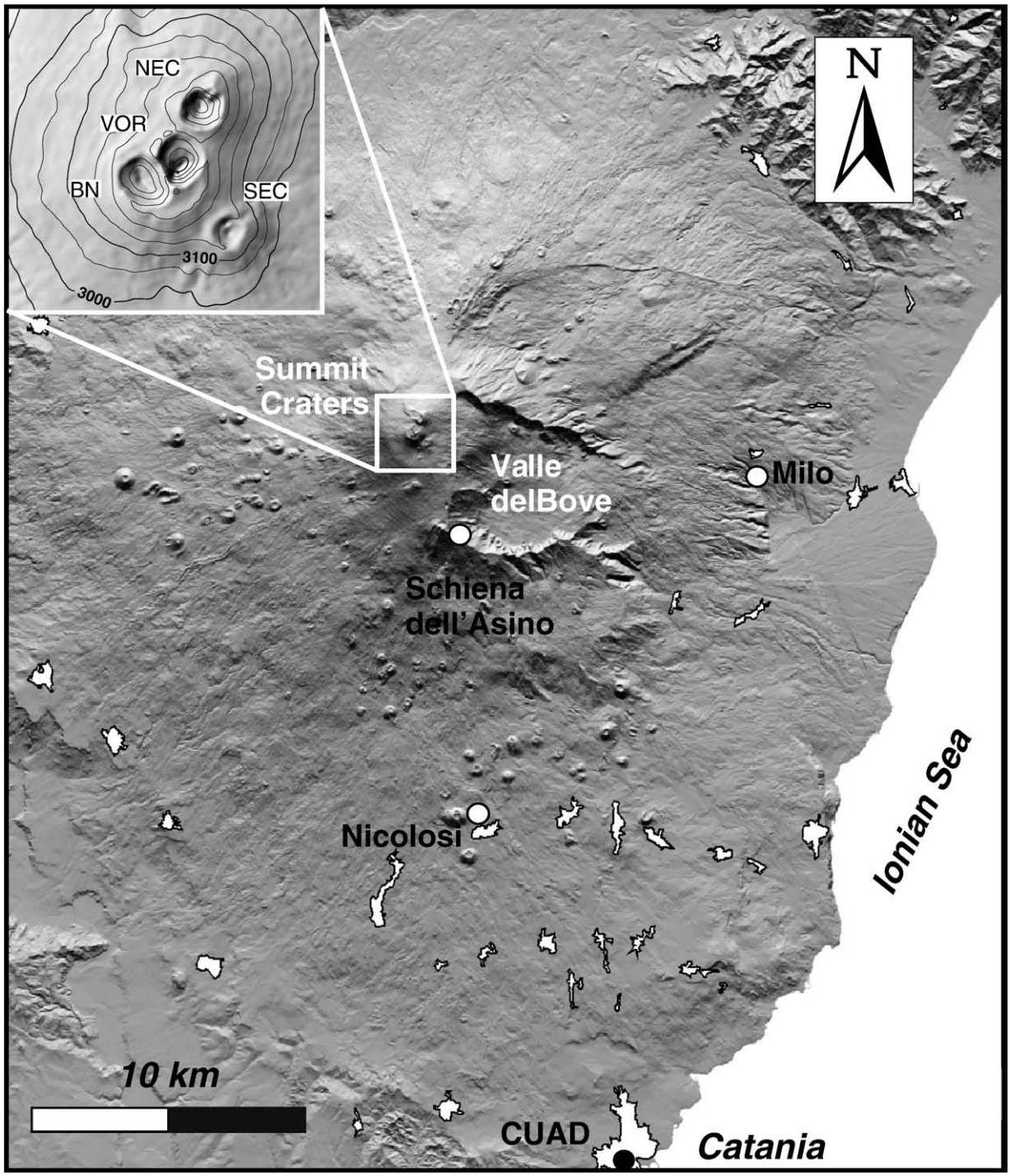

Fig. 1. Map of Mt. Etna. The location of the five cameras of INGV-CT are indicated: Milo, Schiena dell'Asino, Nicolosi and CUAD in Catania (visible cameras), (thermal and visible cameras). The inset shows the summit area and the position of the craters: North East Crater (NEC), Voragine (VOR), Bocca Nuova (BN) and South East Crater (SEC).

plume is often visible even at considerable distances from the volcano, thus often provoking concern for the local air traffic agencies of the civil and military airports of Catania and Sigonella, respectively (Fig. 1).

In this paper, we deal with plumes of differing consistency observed at Etna in 2006, when discontinuous explosive activity caused frequent ash emissions (Andronico et al., 2007a,b, 2009-this issue). A first, short eruption occurred between 14 and 24 July, while a longer eruption lasted from 31 August to 15 December. Especially during the latter eruption, the ash spread from the summit area to a distance of several km away from the volcano, representing a serious danger for aviation. The 2006 episodes of tephra emission lasted from a few hours to days, prompting the need to seek new monitoring techniques to improve forecasting.

Here we present the methodology developed in experiments during and between the 2006 eruptions in order to identify the presence of ash within the volcanic plumes, based on the comparison between visual observations and field data with information provided by the polar constellation of NOAA–AVHRR satellites. Most of the techniques presented in the literature consider only one observation system, either from the ground or satellite. Ground-based surveillance is sometimes inadequate to monitor spatially and temporally large-scale dynamic phenomena, like eruptive ash clouds that spread and disperse in the atmosphere, particularly during cloudy conditions or at night. Conversely, rapid information on the areas affected by evolving ash dispersion is provided by frequent real time acquisition of satellite

images. Nonetheless, limits of remote sensing techniques are well documented (Simpson et al., 2000; Prata et al., 2001; Pieri et al., 2002) and used stand-alone can produce ambiguity in the context of providing operational support of aviation safety (Simpson et al., 2001).

By comparing and integrating ground-based and remote sensing systems, our goal was to enhance the ability of NOAA–AVHRR polar satellite data to effectively detect the sporadic episodes of ash emissions at Etna. After describing the eruptive activity, we present the results coming from the adopted methodology and propose a classification of volcanic plumes observed during 2006. This approach has emphasized the acquisition of real time information on the presence of ash in the volcanic plume. The results obtained by comparing the two observation systems are then integrated into the information stream provided by the Istituto Nazionale di Geofisica e Vulcanologia, Sezione di Catania (INGV-CT), devoted to the monitoring of Etna, in operational support of the Italian Civil Protection. We conclude by demonstrating the advantage of also introducing real-time satellite data into the monitoring system for detecting weak, non-intense ash emissions, like those occurring at basaltic volcanoes such as Etna.

2. The 2006 eruptive activity at Etna

Mt. Etna started erupting during the night of 14 July 2006, when a fissure formed on the eastern flank of the South East Crater (SEC), one of the summit craters of Etna (Fig. 1). Three vents opened along the eruptive fissure at about 3000 m a.s.l., two of them emitting lava flows (joining up after a few hundred meters) that propagated eastwards inside the Valle del Bove (Branca and Consoli, 2006). Between 15 and 23 July, strong Strombolian activity and lava flows were produced from a pit-crater depression located on the east flank of the cone. Although the explosive activity caused ash emission, no formation of sustained eruption columns occurred and tephra fallout was mainly confined over the summit area of Etna. The eruption ended on 24 July 2006; several days of sustained degassing activity without ash emission then took place.

Volcanic activity at SEC recommenced at the end of August 2006, initially due to moderate Strombolian activity. The new eruption ended on 15 December 2006. In this period, a more intense and differentiated eruptive activity affected SEC, characterised by almost continuous explosive activity both at its summit and eastern slopes, and interspersed only by a few temporary vents or minor fractures involving small to significant rock-falls and debris avalanches during paroxysmal activity (e.g., Branca and Polacci, 2006; Norini et al., 2008). From 4 September, short lava flows overflowed from the summit vent eastwards for a few hundreds of meters (Calvari and Lodato, 2006) that stopped in mid-September. A new eruptive fracture opened on 13 October from the East base of SEC, trending ESE–WNW and reaching the altitude of 2800 m a.s.l.; an effusive activity started forming lava flows spreading eastwards and causing quasi-permanent lava flow effusion up to the end of the eruption. Eruptive fractures also opened on the S-flank of Bocca Nuova, emitting lava flows for a few hours on 26 and 28 October (Calvari, 2006a; Coltelli, 2006) and on 16 November (Calvari, 2006b).

On the whole, the August–December 2006 eruption was preliminarily subdivided by Andronico et al. (2009-this issue) into three main *stages*, during which eruptive activity (both explosive and effusive) was characterised by different styles and intensity, hereafter briefly described mainly from the explosive point of view.

2.1. First stage: 31 August–27 October

Seven prolonged episodes (lasting one to several days) of discontinuous, strong Strombolian explosions occurred at SEC, usually forming ephemeral plumes over the summit of Etna. In between these episodes, minor explosions took place at the cone. Minor effusive activity produced short lava flows from the summit and along flank fractures opened on the cone slopes, while a permanent effusive vent-fissure opened at 2800 m a.s.l.

2.2. Second stage: 27 October–27 November

This phase featured eleven main explosive episodes lasting a few to tens of hours, whose intensity increased significantly with respect to those observed during the first stage. Paroxysmal activity often occurred in flank pit-craters that formed in the east part of the cone. This activity usually led to the formation of weak and/or discontinuous ash-enriched plumes above SEC, eventually causing moderate to light tephra showers as far as Catania and other villages around Etna. Effusive activity at the 2800 fracture continued.

2.3. Third stage: 27 November–15 December

After 27 November, the eruptive style changed and SEC was affected by 2–4 day-long episodes of prolonged ash emission. This activity was mainly related to deep and pulsating explosions centred within the main pit-crater inherited from the last paroxysm of 27 November. As a consequence, this style produced low, dense and ashy plumes that rose to altitudes of one–two hundreds of meters above the vent before drifting with dominant winds to form bent and usually narrow plumes over the summit, causing very light but continuous ash fallout over the roads. On some days air traffic was also disrupted even as far as the Reggio Calabria airport, about 70 km north-eastward from the vent.

3. Methodology

The integrated observation approach described in this paper is based on the continuous comparison between data on explosive activity and associated tephra emission on one hand and satellite observation on the other, with the goal of predicting the next ash emission episodes at Etna.

3.1. Ground ash emission data

Monitoring of Etna is performed by INGV-CT which acquires data from different observational systems and geophysical and geochemical networks. At present, ash emissions and associated fallout deposit are monitored by integrating information derived from camera networks, visual observations and from tephra samples (Andronico et al., 2009-this issue). These operations aimed to evaluate the duration and intensity of most of the ash fallout events and eventually magnitude and intensity according to the estimation of the erupted volume.

Most information is collected and analyzed at the operations room of INGV-CT, where the pattern of the seismic tremor is continuously monitored. Each significant variation in tremor triggers a warning, possibly indicating an impending explosive activity (Alparone et al., 2003, 2007). Again in the operations room, images of Etna are transmitted in real-time from the five live-cameras managed by INGV-CT around the volcano (four visible and one thermal; Fig. 1). The visible cameras are located in Catania at CUAD (26 km S from SEC and 35 m a.s.l.), Nicolosi (15 km S and 730 m a.s.l.), Schiena dell'Asino (5 km SSE and 2030 m a.s.l.) and Milo (10 km ESE and 770 m a.s.l.), while the thermal one is located in Nicolosi. The visible cameras are Canon (VC-C4 models) and acquire a 420×350 squared pixel image with 47.5° field of view. The thermal camera is a FLIR ThermoVision® 320 M model and uses an uncooled microbolometer that detects the emitted radiation in the 7.5 to 13 μm band, acquires 320×240 squared pixel images and has a 24°×18° field of view. All the cameras acquire an image every 2 s and transfer the video signal in real time to the operations room, where all the images are stored and published (at a lower frame rate) on the website www.ct.ingv.it. The operations room personnel are there to observe variations in eruptive activity and to eventually advise the volcanologist on-duty. The video-analysis of the permanent camera system is used to compile weekly reports of the eruptive activity at Etna that are published on the INGV-CT website. The camera network greatly helps monitoring potential formation and evolution of eruptive plumes above the summit from different points of view, if the weather conditions are good. Wind

direction and intensity provided from the Meteorological station at Sigonella are used to define the area eventually affected by ash fallout. This whole set of information is used for planning the field surveys to acquire tephra samples and then reconstruct the ash fallout dispersal.

3.2. Satellite data

The INGV-CNT Satellite Receiving Station receives AVHRR (Advanced Very High Resolution Radiometer) data in real-time. The station was installed in Rome at the end of 2004. The tracking antenna is configured for capturing data from the NOAA constellation, which currently comprises 6 polar satellites orbiting over the Mediterranean area. The station is a TeraScan system which integrates hardware and software for automated reception of data from satellites and for data processing (Young, 2006). The multispectral sensor AVHRR on board NOAA satellites acquires digital images in the wavelength range from visible to thermal infrared in five different channels (Gary, 2007). The digital images have 1.1 km of spatial resolution when data are acquired at nadir view (NOAA, 2000). Sicily is covered by NOAA data acquisition frequency of a minimum of 4 passes and maximum of 9 per day, thus permitting day and night observation.

NOAA–AVHRR thermal infrared images have been used to develop a technique for detecting the presence of volcanic ash clouds (Prata, 1989a,b; Wen and Rose, 1994; Prata and Grant, 2001). The technique is the so-called "split window" or Brightness Temperature Difference (BTD) method, and has been used extensively during many volcanic eruptions to identify the volcanic ash plumes and also to discriminate them from meteorological clouds (Self and Holasek, 1995; Schneider et al., 1995; Simpson et al., 2002; Tupper et al., 2004). The method is based on the wavelength dependent differential absorption of earth-emitted radiation measured by the sensor in terms of brightness temperature. The identification of volcanic clouds is based on the difference between the brightness temperatures computed from two thermal infrared channels positioned around 11 and 12 μm. Due to the volcanic ash spectral characteristics in absorbing more strongly at 11 μm than at 12 μm, there will generally be a negative difference for volcanic plumes (larger absorption at 11 than 12 μm) and positive for meteorological clouds (larger absorption at 12 than 11 μm). Thus, below the BTD threshold zero the presence of ash is theoretically identified.

However, this method has limitations as reported by Simpson et al. (2000). The main limitation is that many volcanic clouds are mixed with meteorological clouds in which water vapor, water droplets and ice crystals act to mask the negative BTD volcanic cloud signal. There has been substantial discussion in the literature concerning this effect and whether the BTD method is optimal for aviation purposes (Hufford et al., 2000; Prata et al., 2001; Simpson et al., 2001). The following effects have been demonstrated to change the threshold in a positive BTD: 1) high amounts of precipitable moisture in atmosphere; 2) optically dense clouds; 3) ice coating of volcanic particles; 4) high concentration of aerosols; 5) volcanic particles with radius $>>15$ μm.

In this work, the BTD method has been applied to the real-time NOAA–AVHRR images during the entire 2006 eruption. Comparing the BTD results with ground observations, we determined the best BTD threshold for the detection of Etna volcanic ash plumes for dependable detection of sporadic ash emissions. Visible and thermal images have also been used to better identify the volcanic plume. Once the ash is detected, the BTD method allows the mapping of the associated ash plume or cloud and the calculation of parameters useful for volcanic ash hazard detection and tracking. These parameters are: location, extension, direction and altitude of the plume. The extension is considered as the length and the width of the plume; these values are calculated using the georeferenced images after considering the pixel size of the analyzed data both in thermal and in the visible channels. The georeferenced images are automatically provided by Terascan software. From the georeferenced images, plume location and direction are also obtained. The plume height is estimated by the correlation between plume brightness temperatures and atmospheric profiles (Holasek et al., 1996; Tupper et al., 2003). To this end, we used the standard vertical atmospheric profile provided by the Italian Air Force base in Trapani. If multiple layers have the same temperature, the comparison between the wind direction and the corresponding plume direction identifies the plume layer height. The supplemented wind correlation not only overcomes height ambiguities caused by atmospheric inversions, but also the underestimation due to non-opaque clouds and clouds having emissivity of less than unity.

4. The volcanic plumes observed in 2006

During, and in between, the 2006 eruptions at Etna, we identified a number of volcanic plumes both by volcanological observations and satellite image analysis. The maximum number of observations of volcanic plumes from Etna was obtained during the August–December 2006 eruption.

From the volcanological point of view, a volcanic plume is primarily observed by means of live-cameras and visual observations from around Etna. However, this information often needs to be supported with field data. The quantitative measurements of the characteristics of an ash deposit on the ground is the chief parameter for the identification of different classes of eruptive plumes, and in particular the estimation of fallout rate (e.g., mass/unit area and mass/unit time). A low fallout rate may couple with short or long explosive activity; nevertheless intense fallout may last from minutes up to several hours. With respect to duration, in 2006 most explosive events lasted hours to days. Only in few cases were the explosive events short, but with a sequence of explosions in a few minutes intense enough to produce eruption plumes that rose above and drifted away from the summit. One of the main features of the 2006 activity compared with previous paroxysmal activity of Etna (e.g. fire-fountaining in 2000, flank eruptions in 2001 and 2002–03), was the very low rate of sedimentation by ash fallout.

From the satellite remote sensing point of view, the satellite observation system automatically acquired Etna images during every NOAA satellite acquisition. Images are a square of 40×40 km in dimension and centred at the Etna summit craters (latitude: 37°51.50′; longitude: 14°58.01′). The processing of multispectral images allowed the identification of Etnean volcanic plumes, when their dimensions are greater than the pixel size of the acquired image. The meteorological cloud mask and the BTD method are automatically applied to every image and its relatively small dimension reduced ambiguous cases. Larger images (covering the whole of Sicily) are used when a volcanic plume is detected in the smaller 40×40 km image. Using the Sicily BTD image and the visible channel, the plume parameters, namely plume direction, extension (length and width) and height, are calculated.

During 2006, we observed a number of volcanic plumes related to different typologies of eruptive activity. The comparison between observations from ground and from satellite was crucial to recognize their features in terms of ash and cloud detection by satellite, duration, intensity of the explosive activity and tephra fallout. By combining these qualitative and quantitative data, we propose defining five classes of volcanic plume (Table 1): 1) degassing plumes, 2) ephemeral plumes, 3) long-lasting and weak intensity plumes, 4) plumes produced by middle eruptive intensity, and 5) long-lasting and pulsating plumes.

4.1. Degassing plumes

Degassing plumes are the ordinary type of plume that we have become used to seeing over the volcano summit. From a satellite perspective, an intermittent plume was present throughout the period 19–31 July (see Appendix). These plumes were detected in visible channel images indicating that they were mostly composed by the volcanic aerosol (Spinetti et al., 2003; Spinetti and Buongiorno, 2007). The plume was predominately in the south-east quadrant in 50% of observations, while in the south-west quadrant it was observed approximately 30% of the time. No ash plume was identified by the BTD method from AVHRR data.

During the 14–24 July 2006 eruption, satellite images clearly showed the formation of degassing plumes above and away from the summit area of Etna. These sometimes caused the emission of tephra falling around the

Table 1
Summary of the five classes of eruption plumes studied in this work

Class number	Definition	Study case during 2006	Ash detection by satellite	Duration	Eruption typology	Tephra fallout	Notes
1	Degassing plumes	27 July	No	Hours to days	No activity, only intense degassing	No	During quiescent periods and mainly after eruptive activity
2	Ephemeral plumes	31 July	Discontinuous	Tens of minutes to a few hours	Short, low intensity explosive activity	Light shower up to tens of km from the vent or limited to the summit slopes of the volcano	Difficult to capture by satellite
3	Long-lasting and weak intensity plumes	16 November	Continuous	Hours	Moderate to strong Strombolian explosions	Moderate fallout of ash up to tens of km from the vent	The wind rotation can cause wider plume extension and ash dispersal
4	Plumes produced by middle eruptive intensity	24 November	Continuous	Hours	Strong Strombolian explosions to lava fountaining activity	Formation of almost continuous tephra deposit on ground	The wind rotation can cause wider plume extension and ash dispersal
5	Long-lasting and pulsating plumes	6 December	Continuous	Hours to days	Prolonged, pulsating, low intensity explosive activity	Light to moderate, continuous ash fallout	The wind rotation can cause wider plume extension and ash dispersal

explosive vent. However, no ash fallout was observed at greater distances from the volcano. Fig. 2 shows an example of the plume captured early in the morning of 22 July after a consistent explosive activity (starting in the late evening of 21 July at SEC) causing moderate tephra fallout up to a few hundreds of meters from the eruptive vent. In the volcanic plume ash was not detected in either volcanological observations or in satellite data. At 5:39 GMT of 22 July, the plume reached a distal extension of 230 km from the craters and a width of 30 km, then sharply diminished in size following a marked drop in the Strombolian activity (Appendix).

A few days after the end of the July 2006 eruption, SEC and the other summit craters together produced a powerful whitish plume. Fig. 3 shows the 27 July degassing plume from satellite (at 4:57 GMT; Fig. 3a) and from Catania (at 5:00 GMT; Fig. 3b), and finally a few hours later just from the summit western slope of the volcano (Fig. 3c). The plume reached a maximum distal extension of up to 250 km.

4.2. Ephemeral plumes

The ephemeral plumes are due to eruptive activity showing low eruptive intensity and short duration, usually lasting tens of minutes to a few hours. These explosions at vents and associated tephra emissions usually resulted in the formation of ephemeral plumes as gauged by the total amount of erupted ash. This kind of plume has been observed by NOAA–AVHRR only in sporadic cases, as their dimensions have often been equal or smaller than the size of the detected pixels. In applying the BTD method to the AVHRR Etna image (that's 40×40 km), only a few episodes of ash emission have been identified in the summit area.

We present two different examples occurring on 31 October and 8–9 November. On 31 October, an abrupt short sequence of discrete, powerful Strombolian explosions, started at 11:45 and ended at 13:00, producing a dense but spatially confined ash plume that shifted toward the west (Cristaldi and Scollo, 2006; Fig. 4). Although this plume reached a height of a few hundreds of meters above the vents, it formed a modest deposit in the upper slopes of Etna. During this event, the presence of ash was detected by BTD at 12:05 (Appendix).

The last ephemeral plume was produced by weak Strombolian explosions that began at SEC on 8 November afternoon (Andronico and Scollo, 2006). This activity ended in the morning of 9 November. Also on this occasion, the fallout was so light that it was scarcely perceived by the local population, causing a deposit less than 1 g/m^2 at Bronte (at about 15 km NW of Etna). AVHRR data clearly showed an ephemeral plume at 05:04 GMT of 9 November (Fig. 5), notwithstanding that the BTD didn't identify the plume as containing ash.

4.3. Long-lasting and weak intensity plumes

During the August–December eruption, SEC produced many ash plumes originating from long-lasting and weak intensity eruptive activity. We show a case study that occurred during the paroxysm of 16 November, characterised by strong Strombolian activity, rock-falls and debris

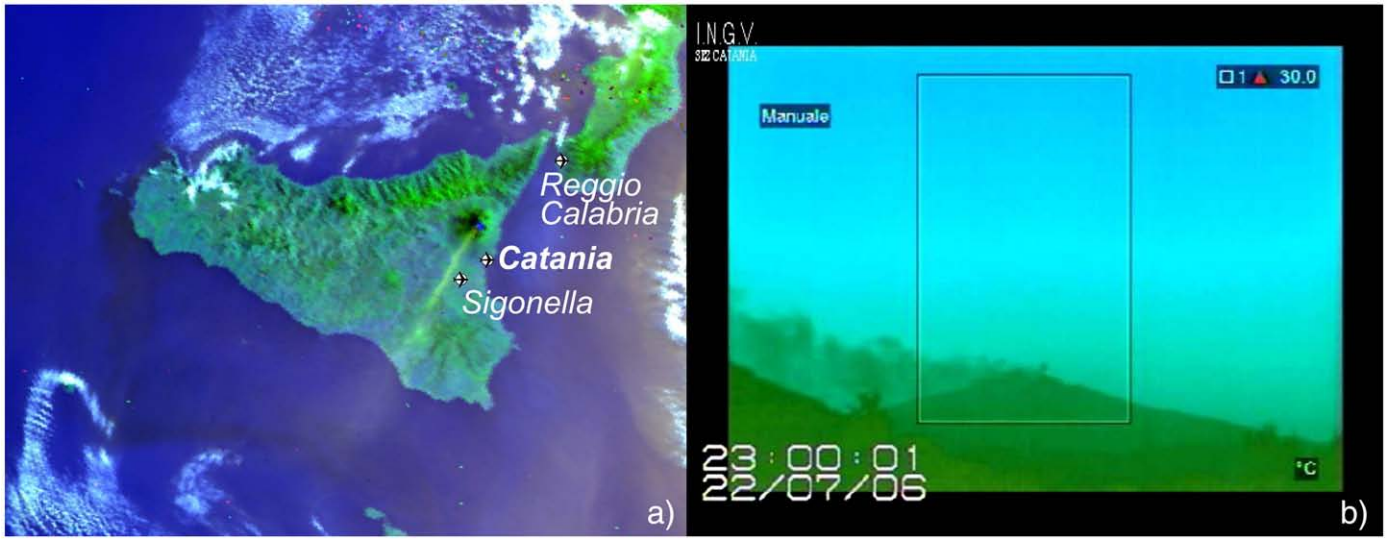

Fig. 2. The 22 July 2006 degassing plume observed: a) from satellite NOAA–AVHRR at 5:39 GMT (RGB composition), and b) from the Nicolosi thermal camera at 23:00 GMT. In a) the main urbanised areas (with airports) reported in the text are indicated: Reggio Calabria, Catania and Sigonella.

Fig. 3. The 27 July 2006 degassing plume observed: a) from the summit western slope of the volcano at 10:00 GMT; b) from Catania downtown at about 5:00 GMT (at a distance of about 28 km southward from the eruptive vent); (c) from satellite NOAA–AVHRR at 4:57 GMT (RGB composition).

avalanches (see also Andronico et al., 2009-this issue; Norini et al., 2008) for at least 10 h between 06:00 and 14:00 GMT. This complex activity caused a composite, although inconsistent tephra plume and light ash fallout on the NE sector of the volcano. Fig. 6 shows the volcanic plume as viewed from the south, from the direction of Catania at different distances. The 16 November 2006 plume rose to approximately 1 km above SEC and produced a moderate deposit at 15–20 km from the vents of <5 g/m^2. Satellite observations revealed the ash presence in the plume at 8:26 and at 19:51 GMT; however the rest of the time meteorological clouds masked the plume. This plume was spread around the summit area with a width of 7 km reaching up to 3900 m a.s.l. after its onset (Appendix).

4.4. Plumes produced by middle eruptive intensity

The fourth class includes nearly sustained volcanic plumes like those occurring on 21 and 24 November. During these events, paroxysmal activity ranged between strong Strombolian and lava fountaining, causing the formation of a more consistent eruption plume above the summit of Etna than those previously formed. Here, we describe in particular the 24 November episode, which was probably the most intense paroxysm in 2006 according to its tephra fallout (Andronico et al., 2007a, 2009-this issue). The eruptive activity started at 6:00 GMT and almost immediately it was able to form a plume that was blown toward the SE by winds at that time (Fig. 7). The paroxysm lasted until 15:00 GMT, when it abruptly declined, and then ended. During almost 10 h of activity, the rotation of the winds caused the shifting of the plume (and consequently of the fallout) to the south. The eruption column rose to a height of approximately 1.3 km over the Etna summit and produced a nearly continuous deposit on land over the middle slopes of the volcano and a discontinuous deposit in the city of Catania. The fallout rate, however, was not intense: 50–70 g/m^2 fell along the Ionian coast between Acireale and Catania, over a fallout time of about six hours (the plume was rotating), indicating a fallout rate of about 5–6 g/m^2 h^{-1}. The satellite images documented an ash plume rotation from SE to S, resulting in a wider plume (16–30 km) between 11:00 and 15:00 GMT with respect to before and after (less than 5 km; Fig. 8). The

Fig. 4. The 31 October 2006 ephemeral plume observed from the Schiena dell'Asino visible camera at 12:00 GMT.

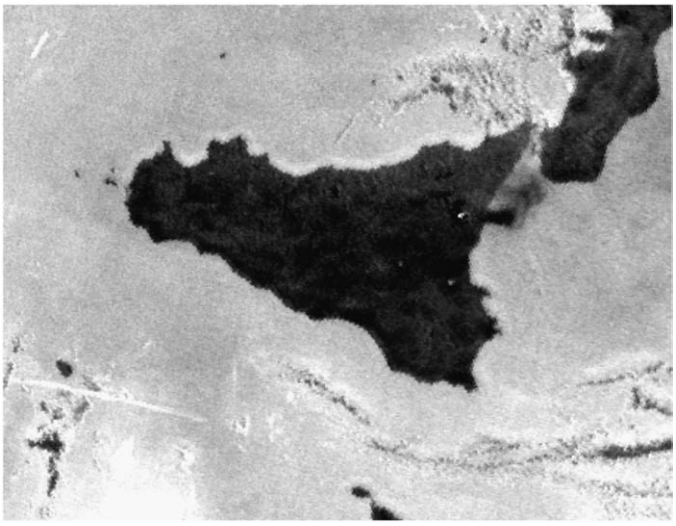

Fig. 5. The 9 November 2006 ephemeral plume observed from satellite at 05:04 GMT.

plume altitude was between 4900 to 5400 m a.s.l. from 10:00 to 11:20 GMT. The maximum plume length was estimated as 338 km (distal ash identified at up to 83 km from the vent) at 11:20 GMT, while the maximum width resulted 82 km at 15:15 GMT (ash presence identified up to 30 km) (Appendix).

4.5. Long-lasting and pulsating plumes

During the 27 November paroxysm, a pit-crater formed in the eastern side of SEC. This pit was the location of continuous (although low intensity) explosive activity, that generated bent and narrow plumes during the last phase of the August–December 2006 eruption (27 November–15 December). In this period, however, the presence of meteorological clouds limited the observation both from the ground camera network and from satellite. Tephra deposits on land were very light and discontinuous due to the continuous shifting of the winds coupled with the low ash content. Fig. 8 shows the volcanic plume as it appeared on 6 December. In this case, the plume was poorly defined, laterally well dispersed and relatively short, probably not only because of the low level of explosive activity, but because of weak winds in the morning (5 knots at 3000 m a.s.l.). The plume altitude was between 3600 and 4600 m a.s.l. at 5:37 GMT. In other cases, as on 4 December, the plume was weaker in the morning and then grew due to increasing intensity of explosions (Appendix). This factor, together with an increase of wind intensity, caused the formation of an elongated plume in the evening, resulting in a light shower of fine ash over the town of Reggio Calabria (Fig. 9).

5. Discussion

We have conducted continuous observations of the volcanic plumes formed during eruptive activity from Mt. Etna by routine use of live-cameras and traditional volcanological field observations. During 2006, for the first time, Etna volcanic plumes were observed in real time both from satellite and from the ground simultaneously and results from each detection method were compared. In the period July–December 2006, in particular, the introduction of satellite data into the observation systems of Etna was of significant use to detect the presence of ash clouds in the atmosphere. In many cases (but not always), the 2006 plumes contained volcanic ash (Appendix). The main factors on whether or not there was a detectable presence of ash in the observed volcanic plumes were the duration and the intensity of the eruptive activity, while the strength and direction of the winds mostly influenced the areas where ash was dispersed.

5.1. Classification of volcanic plumes

Information on the presence or lack of ash in atmosphere (based on satellite images and visible and field data) allowed us to identify five classes of volcanic plumes, with the potential to infer the level of eruptive hazard. For ease of reference and identification, in the following section and in Appendix, we will define and refer to our five plumes as Class 1 through Class 5.

Class 1 includes *degassing plumes* that are not heavily loaded with ash. Matsushima and Shinohara (2006) divided such volcanic plumes into two distinctive categories according to their appearance. The first category includes transparent, invisible plumes that are composed of volcanic gases, while the second class is formed by visible plumes that contain aerosols and water droplets in addition to the gases. These authors highlighted that parameters controlling the visibility of volcanic plumes, including the exit temperature of the volcanic gas, the gas composition (HCl and H_2O), atmospheric temperature and humidity. At the same atmospheric condition the lower exit temperature induces the formation of opaque plumes for lower gas mole ratio (HCl/H_2O) and vice versa for transparent plumes. The degassing transparent-type plume is normally present at Etna since it is a quiescent volcano. The distal plume is often confined within a few to tens of km from the summit craters (Spinetti et

Fig. 6. The 16 November 2006 long-lasting and weak intensity plume observed from Catania downtown at 15:30 GMT. Mt. Etna is covered by the meteorological clouds and the plume overcomes it and directs towards east on the right of the picture.

Fig. 7. The 24 November 2006 middle eruptive intensity plume observed: a) from the Catania visible camera at 06:00 GMT; b) from the Nicolosi thermal camera at 06:00 GMT; c) from Catania (INGV-CT, at about 27 km southward of distance from the eruptive vent) at 08:00 GMT.

al., 2007). This kind of plume is generally absent in AVHRR data and also not detectable from the ground-based thermal camera network. Significant examples of individual opaque-type plumes were observed in AVHRR data between 19 July and 20 September 2006, suggesting a greater degassing than usual. The combination of the gases at higher temperature and the summer atmospheric humidity produced an opaque plume mainly composed of aerosols. The observed heterogeneity in the aerosol composition suggests that fine ash often co-exists with water and acid droplets. Indeed, such plumes may necessitate warnings for air traffic due to the inability of ruling out the presence of ash and acid aerosols, both of which potential threats to reciprocating and turbine aircraft engines (Tupper et al., 2006). In addition, at Etna measurements of the SO_2 content within this kind of plume is retained basic for surveillance purposes. Since October 1987, in fact, the monitoring of plumes degassing from the summit craters has been periodically carried out by a mobile correlation spectrometer (COSPEC) (Bruno et al., 2001 and reference therein), and although acquired with different techniques and sampling frequencies, measurements often proved useful to estimate possible ascent and shallow emplacement of magma at Etna.

Plume classes from 2 to 5 may constitute a real volcanic hazard. The *ephemeral plumes* (class 2) are usually too short and small to be detected by a satellite system. Their briefness makes them more hazardous in the confined summit area, but they can produce light ash fallout at considerable distances from the volcano summit.

Class 3 includes *long lasting but weak intensity plumes*. This kind of plume is ash-poor, however, it may have as much ash injection potential. The long duration of eruptive activity, in fact, compensates for the low rate of ash emission and subsequent low rate of fallout. In 2006, these plumes were usually gas-enriched and contained fine ash. This feature of the plume is important, because the finer the ash, the longer the atmospheric residence time in air and the time required for fallout (Sparks et al., 1997).

Class 4 proved to be one of the most hazardous of the ash plumes during 2006. *Middle eruptive intensity plumes* have prompted cessation of air operations, not only because of the formation of constant plumes, but also for the greater tephra fallout with respect to the previous classes. These plumes were associated with paroxysmal events including strong Strombolian and lava fountaining activity lasting a few to ten hours, and formed a continuous to almost continuous ash cover on the ground.

Class 5 includes *long lasting and pulsating plumes* that were formed by an eruptive activity not commonly observed at Etna, at least within the last few years. However, these plumes produced an impact in terms of ash fallout similar to plumes of the previous class 4 (*middle eruptive intensity plumes*). The main difference is the lower eruptive rate due to an intermittent and lower explosivity, that has caused the formation of elongated and narrow plumes in case of mid-high intensity wind, or, conversely, a shorter wide cloud above the volcano in case of lower velocity winds. Similarly to plumes from the class 3 (*long lasting but weak intensity plumes*), the main hazard was related to the duration that was

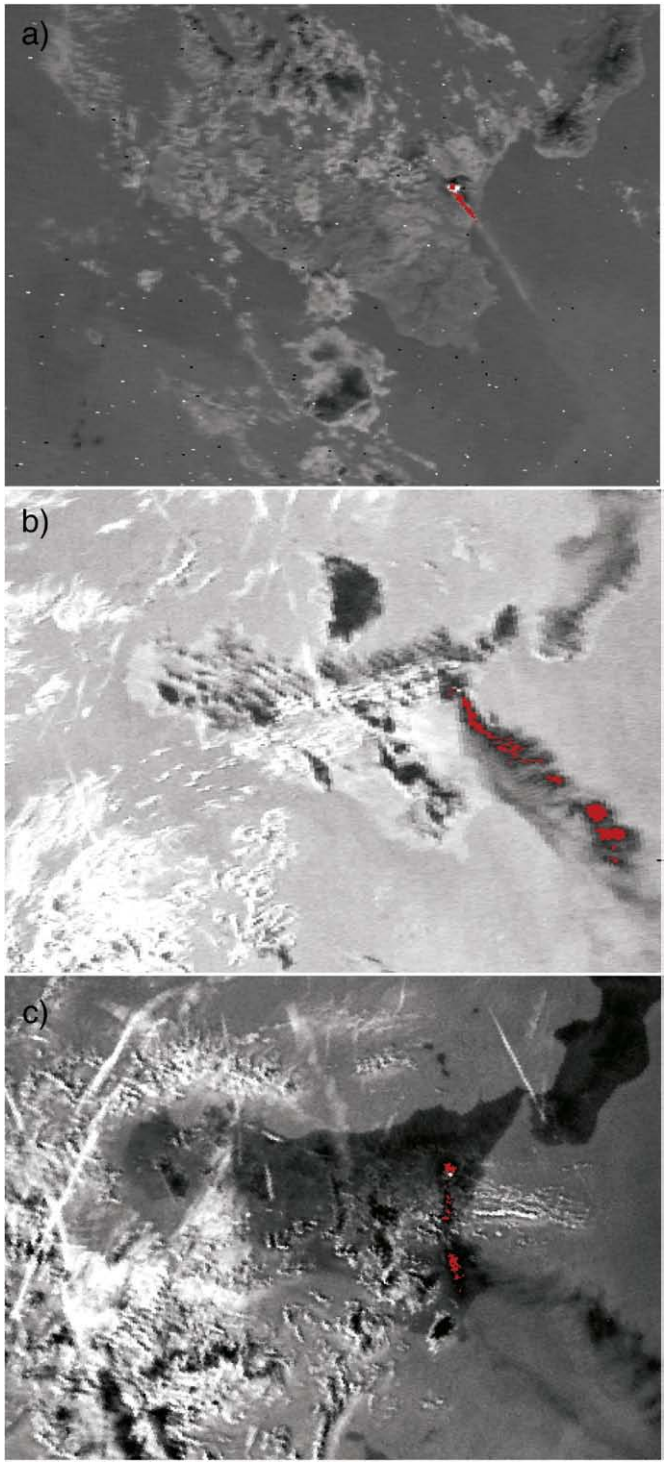

Fig. 8. The 24 November 2006 middle eruptive intensity plume observed from satellite at: a) 08:22 GMT; b) 13:00 GMT; c) 15:14 GMT.

extremely long (up to 3 days). The presence and variability of persistent winds also increased the volume of air space contaminated by volcanic ash plumes and areas impacted by ash fallout. This is the case of the 12 December plume, that was able to reach the Calabria region to the north-east, causing disruption to the local airport at Reggio Calabria.

5.2. A satellite system for monitoring purposes: advantages and limits

The Etna plumes detected by the polar satellite NOAA–AVHRR from July to December 2006 have been compared in this paper with those recognized by means of the visible surveillance, as shown in the Appendix. This comparison evidences the difference between the two observation systems. The satellite information has identified large plumes and their extension area thanks to the wide and fast view that satellite permits. In the Appendix, the visible and thermal identification of plume from orbit is shown together with data on plume extension (length and width), plume altitude and information on ash presence.

Ash identification has been possible by applying the BTD method in a systematic way to the AVHRR image data over the Mt. Etna region. This method produces identification of volcanic ash clouds during almost the

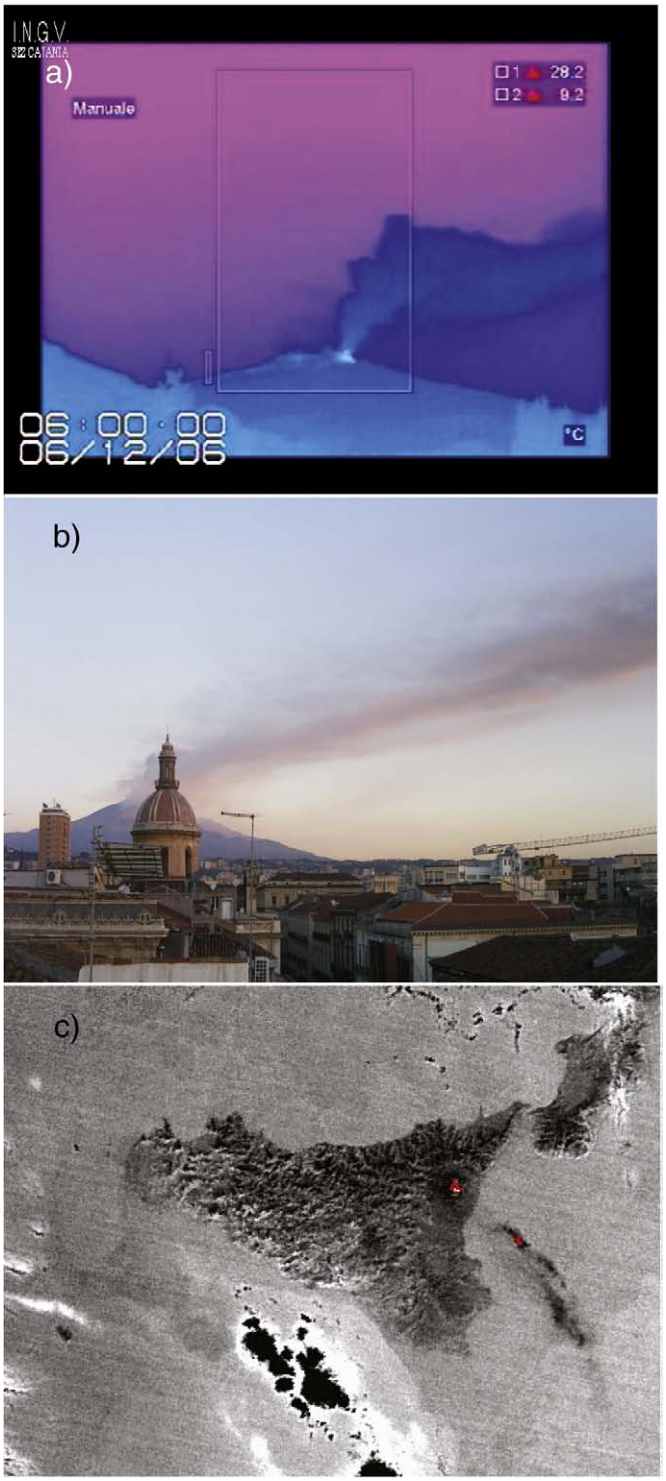

Fig. 9. The 6 December 2006 long-lasting and pulsating plume observed: a) from the Nicolosi thermal camera at 06:00 GMT; b) from Catania downtown at 06:00 GMT; c) from satellite at 09:04 GMT.

entire data set analyzed in 2006 when meteorological clouds were absent. The identification is confirmed by traditional volcanological observations and field sampling. With respect to our plume classes, the BTD method shows that the lower the assigned class numerical ranking, the more negative are the BTD values, except for class 1. We found that for classes 2 and 3 the BTD threshold is −1, thus the sporadic ash emission identified using AVHRR corresponded well to what was observed on the ground. Conversely, classes 4 and 5 are typically associated with a BTD threshold of −0.2. Therefore, different classes occur under different atmospheric conditions, from summer to winter, suggesting that the threshold is related to local atmospheric conditions, mostly influenced by the water vapor variability (Pieri et al., 2002; Yu et al., 2002). Moreover, negative values can produce ambiguous cases in volcanic ash identifications when meteorological clouds are present (Prata and Grant, 2001). Our data analysis also indicates that some meteorological clouds have negative BTD values, especially in the winter. The ice presence in the meteorological clouds gives similar values to volcanic clouds (Simpson et al., 2000; Prata et al., 2001). It should be noted that high atmospheric water vapor and low ash concentration affect the BTD method in yielding positive values for ash plumes (Prata et al., 2001), as occurred for the 9 November 2006 ash emission. We mentioned also that pixels containing barren or vegetation-poor land can give negative BTD values. In the elaboration of the whole images of Sicily these pixels are easily identifiable and excluded as non-volcanic ash cloud by their shape and location impossible to be reached by ash following the wind direction. A different technique (Pergola et al., 2004), based on the BTD method combined with AVHRR historical series, allows the possibility of better differentiating the presence of volcanic ash, thus reducing somewhat the number of ambiguous cases, even though a number of common problems still remain unsolved for an automatic ash detection scheme (Filizzola et al., 2007).

Our detailed examination of the five defined classes has shown that at present satellite detection schemes have limits in recognizing the formation of eruptive clouds. The main limit is the sparse repetition time of polar satellites, which may not allow the detection of sporadic or short duration plumes. For example, most plumes of class 2 (*ephemeral plumes*) were not observed in time. To overcome this limitation, more frequent satellite observations are required. To this end, the use of the geostationary satellite MSG-SEVIRI (Meteosat Second Generation-Spinning Enhanced Visible and Infrared Imager) would improve the frequency of observation (every 15 min, for instance), but the SEVIRI spatial resolution of 3 km limits the detection of volcanic plumes as small as than those detected by AVHRR (spatial resolution of 1.1 km). The MSG-SEVIRI has identified the eruptive plume for only a few major events of class 4, as occurred on November 24th (Spinetti et al., 2008). These few events were detected and recorded by the Toulouse Volcanic Ash Advisory Center (http://www.meteo.fr/aeroweb/info/vaac/homepage/evaa.html).

Even given an ability to detect short duration volcanic plumes, a further limit is the presence of meteorological clouds that are not distinguishable by the BTD method. In these cases, most of the volcanic plumes were identified when they clearly extended beyond or reached a higher altitude than the meteorological clouds, as occurred on 24 November 2006.

The rotation of the source direction of wind during the eruptive activity may distort the perception of the volume of a volcanic cloud, also. The 24 November 2006 case study shows the result of a plume lasting several hours in conditions of significant variations in wind direction. The initial visual and satellite images clearly showed a narrow plume trending about SE. The clockwise wind rotation also caused the rotation of the plume southward with time. In satellite images this was manifested as a disconnected eruption cloud, no longer being fed by the eruption. Satellite data revealed an ash-enriched plume apparently larger than previously observed. Fig. 8 evidences that the initial, 08:22 GMT narrow plume (Fig. 8a) appeared significantly enlarged in the following hours (at 13:00 and 15:14 GMT in Fig. 8b and c, respectively) because when rotating, the wind dispersed the cloud that remained "suspended" in the air for tens of minutes to some hours before dissolving. This apparent enlargement caused the perception of a higher eruption activity from the ground in terms of tephra production and related fallout. A time sequence of satellite images would help distinguish a wider plume due to an increasing activity rather than due to the rotation of the plume.

Finally, one of the main pieces of data required soon as possible during an eruption crisis is the exact time of the onset of the eruptive activity and therefore the timing of the plume formation. In addition, plume spatial extent data provided by satellite observation are important as boundary conditions for models that forecast the rate and location of plume dispersion. Information such as column height and drift directions of the plumes constitute input data for dispersal modelling in time and space. Also, an important goal for such a remote sensing system should be the quantification of the ash burden within the plumes, another key issue for numerical models. Indeed, the concentration of ash, together with the variation of concentration away from the vent along the eruption cloud, determines the level of hazard from tephra fallout, as well as the potential hazard to aviation operations near the area affected by the eruption.

6. Conclusions

Volcanic plumes signal the intensity of eruptive activity and thus data describing the plume are an important component of volcano monitoring. Satellite remote sensing is a powerful tool that provides useful information in this regard. It is complementary to other monitoring techniques, which, taken together, can promptly warn of impending ash clouds and reduce the risk for aircraft. A multidisciplinary approach is required to improve our ability in tracking eruption clouds in the atmosphere, involving field volcanologists together with those who analyze satellite data and who study dispersal models. The integration of these diverse skills will clearly contribute to providing information and strategies to hazard responders who are charged with the mitigation of the hazard from volcanic plumes.

This paper is a step toward the systematic use of satellite data to provide direction, height, width and length of volcanogenic plumes in near real-time. During 2006, at Etna we had the opportunity to compare the satellite detection efforts and the ground observation. This comparison allowed scrutinising ash plumes produced by sporadic eruptive events, demonstrating the advantage and limits of combining ground and orbital observations for such events.

The five different plume categories need to be better developed quantitatively, and may constitute a tool to indicate the occurrence of ash within plumes, thereby giving a more realistic hazard assessment to authorities, possibly decreasing or avoiding unnecessary airport closures.

Future work will better address the comparison between satellite and ground data. For instance, the latter could be made more effective by implementing a real-time acquisition of the ash fallout in terms of accumulated fallout mass by developing a network of balances deployed in the field. Finally, satellite plume detection techniques should be more promptly integrated within the hazard response process. We feel strongly that the synergy of the two observational approaches—ground and orbital—will markedly improve the effectiveness of mitigation responses by both the volcanology and the Civil Protection communities.

Acknowledgements

We thank the Unità Funzionale Sala Operativa for their excellent management of the camera network of the INGV-Sezione di Catania and all those that helped in collecting ash and providing information on tephra fallout. This work was partially supported by the FIRB B5 Italian project "Sviluppo Nuove Tecnologie per la Protezione e Difesa del Territorio dai Rischi Naturali" funded by MIUR. We thank the LABTEL-CNT group for satellite system maintenance, and particular thanks to Dr. J. Dean and Dr. R. Skogg for providing the AVO system. Prof. D. Pieri is greatly thanked for his thorough reviewing, especially in the editing of the paper, which has improved the work considerably. The authors are grateful to two anonymous referees for their appreciation, and particularly to one of them that provided useful suggestions and constructive comments. Finally, we sincerely thank S. Conway for his precious help in editing the paper.

Appendix

List of the Etna volcanic plumes detected by satellite NOAA–AVHRR with the relative information on plume dimensions and volcanic ash presence together with ground observations in the period from 1 July – 31 December 2006. The "Plume classification" has been reported when both observative systems (from ground and from satellite) contributed to detect the type of plume. The numbers correspond to the following classification: 1: Degassing plumes; 2: Ephemeral plumes; 3: Long-lasting and weak intensity plumes; 4: Plumes produced by middle eruptive intensity; 5: Long-lasting and pulsating plumes. CT = Catania; UA = urbanized areas; D. AV. = debris avalanche.

Date	Time GMT (hh:mm)	Satellite plume observed in visible (V) and/or thermal (T) AVHRR channels	Plume direction	Plume extension length–width (km–km)	Ash plume extension (km–km) or clouds satellite observation (hh:mm)	Min-max altitude of plume top (m a.s.l.)	Ground plume observation (G) and camera visible detection (C)	Plume classification
19-07-2006	05:11	V	SSE	36–18	Some clouds		G, C	1
20-07-2006	04:31	V	SSW–SSE	250–10			G, C	1
21-07-2006	06:05	V	SW	180–10			G, C	1
21-07-2006	10:02	V	SW	50–7			G, C	1
22-07-2006	05:39	V/T	SW	230–30/10–2		3300	G, C	1
22-07-2006	09:36	V	SW	70–3			G, C	1
22-07-2006	12:36	V/T	SW	40–3/ 21–3		3300	G, C	1
23-07-2006	04:56	V	S	70–15			G, C	1
24-07-2006	04:31	V	NNE	30–5			G, C	1
25-07-2006	04:07	V	SE	200–15			G, C	1
26-07-2006	05:44	V/T	ESE	60–25/30–6		3300	G, C	1
27-07-2006	04:57	V	SE–S–SE	250–25			G, C	1
28-07-2006	04:58	V	S	50–15			G, C	1
29-07-2006	13:01	V	SE	60–12			G, C	1
30-07-2006	05:23	V	ESE	150–8	Clouds (05:23–11:14)		G, C	1
30-07-2006	15:32	V	SE	120–12			G, C	1
30-08-2006	05: 12	V	ESE	70 7			G, C	1
01-09-2006	05:08	V	SSE	90–30			G, C	1
02-09-2006	05:39	V	SWS	50–7			G, C	1
03-09-2006	05:16	V	SW	50–5			G, C	1
04-09-2006	15:15	V	SSW	15–2			G, C	1
04-09-2006	16:14	V	SW	20–2			G, C	1
05-09-2006	05:09	V	WSW	40–10			G, C	1
06-09-2006	05:42	V	SW	40–7			G, C	1
07-09-2006	05:21	V	S	30–3			G, C	1
08-09-2006	04:57	V	SE	72–5			G, C	1
20-09-2006	05:11	T	SE	50–5		3300–3500	G, C	1
07-10-2006	05:06	T	SE	15–2		3400–3800	G, ash plume	2
07-10-2006	05:19	T	SE	40–4		3400–3800	G, ash plume	2
10/11-10-2006	22:00/22:00		S SE		Clouds 9:29–20:56		G, C; fine ash in Ct	
12-10-2006	09:16				<1.1–<1.1			2
12-10-2006	20:42				<1.1–<1.1			2
13-10-2006	20:30				<1.1–<1.1			2
22-10-2006	06:00–18:00				Clouds 8:47–20:13		C; plume formation; discontinuous ash emission	
23-10-2006	20:00				<1.1–<1.1			
24-10-2006	05:00	T		3.3–3.3	3.3–3.3	3500–3900		
25-10-2006	08:29				Clouds 04:34–16:00		G, C: observation of plume in summit area	
25-10-2006	21:12	T	SE	27–5		3300–3600		
26-10-2006	04:10				<1.1–<1.1		G, C	3
26-10-2006	09:31	V	NW	3–1		3300		
27-10-2006	20:49				<1.1–<1.1			
28-10-2006	05.04				<1.1–<1.1			
28-10-2006	09.10				<1.1–<1.1			
29-10-2006	08.57				<1.1–<1.1			
29-10-2006	15:00–15:30		S SE		Clouds 12:25–21:14		G, C; ash fallout in CT	2
29-10-2006	16:04	T	S SE	42–3		3300	Some clouds	2
30-10-2006	04.11				<1.1–<1.1		Clouds 8:44–15:30	
30-10-2006	15:31				<1.1–<1.1		Some clouds	
30-10-2006	20:10				<1.1–<1.1			
31-10-2006	00:38				<1.1–<1.1			
31-10-2006	03:47				<1.1–<1.1			
31-10-2006	11:45–12:15		S SE				G, C; ash fallout in CT	2
31-10-2006	12:05				<1.1–<1.1			
05/06-11-2006	20:00/05:00		E		Clouds 20:33–12:44		G, C; ash fallout in UA	2
06-11-2006	15:58				<1.1–<1.1			
07-11-2006	04:14				<1.1–<1.1			
08/09-11-2006	12:00/08:00		NW				G, C; ash fallout in UA	2
08-11-2006	15:09				<1.1–<1.1		C; clouds	3
08-11-2006	19:54	T		4–1	4–1	3300	C; clouds	3

(continued on next page)

Appendix (*continued*)

Date	Time GMT (hh:mm)	Satellite plume observed in visible (V) and/or thermal (T) AVHRR channels	Plume direction	Plume extension length–width (km–km)	Ash plume extension (km–km) or clouds satellite observation (hh:mm)	Min-max altitude of plume top (m a.s.l.)	Ground plume observation (G) and camera visible detection (C)	Plume classification
09-11-2006	00:46				<1.1–<1.1		C; clouds	3
09-11-2006	05:04	T	E NW	31–9		3300	C; clouds	3
11-11-2006	09:29	T	N	3–1	3–1			
11-11-2006	11:52				<1.1–<1.1			
16-11-2006	05:10–20:00				Clouds 10:06–15:12		G, C; D. AV.	3
16-11-2006	8:26	T	NE	6–4	6–4	3400–4300		3
16-11-2006	19:51	T	NE	7–5	7–5	3300–3900		3
19-11-2006	04:00–14:00				Clouds 00:44–20:53		G, C	
21-11-2006	12:00–00:00				Clouds 09:21–16:59		G, C; storm rain, clouds	4
21-11-2006	20:27	T	E NE	45–5		4300–4500	G, C	4
21-11-2006	20:54	T	E NE	65–5		4000–4300	G, C	4
22-11-2006	00:13	T	E NE	15–9	Some clouds	3300	G	4
24-11-2006	08:22	V/T	SE	238–12	18–3	4300–4500	G, C	4
24-11-2006	10:02	V/T	SE	300–18	45–5	4900–5400	G, C	4
24-11-2006	11:20	V/T	SE	338–22	83–16	4900–5400	G, C	4
24-11-2006	13:01	V/T	SE	224–54	54–30	4700–4900	G, C	4
24-11-2006	15:14	T	S	275–82	18–2 some clouds	4300–4500	G, C	4
25-11-2006	05:08	T	SE	28–3		3300–3700	G, C	3
25-11-2006	05:41	T	SE	28–3		3300–3700	G, C	3
26-11-2006	01:12	T	S SW	30–2	30–2	3600–4200		
26-11-2006	04:43	T	S	15–2	15–2	3600–4200		
26-11-2006	05:17	T	S	28–2	28–2	3600–4200	G	3
26-11-2006	16:35	T	SW	8–2	8–2; clouds 01:02–20:18	3600–4200	G, C; storm rain	3
27/28-11-2006	10:00/04:00				Clouds 01:02–20:18		G	
29-11-2006	14:51	T	SW	15–2	Some clouds 15–2	3300–5000	G, C	5
29-11-2006	21:09	T	SW	10–2	Some clouds 88–5	3300–5000	G, C	5
30-11-2006	00:31	T	W SW	13–2	Some clouds 60–4	3300–3900	G, C	5
30-11-2006	05:22	T	W SW	11–2	Clouds 08:45–16:44	3300–3900	G, C	5
30-11-2006	20:10	T	W	33–5	Some clouds 33–5	3800–4400	G, C; ash fallout in UA	5
01-12-2006	00:21	T	W SW	37–15	42–50	4200–4300	G, C	5
01-12-2006	04:21	T	SW	20–4	62–14	3300–3900	G, C	5
01-12-2006	04:58	T	SW	9–2	59–16	3300–3900	G, C	5
03-12-2006	05:50	T	E SE	75–15		8–2	G, C	5
03-12-2006	13:09	V/T	E SE	90–7 30–3	Some clouds	3300–3700	G, C	5
03-12-2006	14:52	T	E SE	20–2		3300–3700	G, C	5
03-12-2006	16:32	T	E SE	15–2		3300–3700	G, C	5
04-12-2006	16:07	T	SE	75–4	10–4 clouds 05:27–16:07	3300	G, C	5
04-12-2006	16:50	T	SE	45–4	12–2	3300	G, C	5
04-12-2006	19:23	T	SE			3300	G, C	5
05-12-2006	01:20	T	SE			3300	G, C	5
05-12-2006	09:20	T	S SE			3300	G, C; clouds	5
05/06-12-2006	22:00/11:00						G, C	5
06-12-2006	05:37	T	SE	20–2	Clouds 15:17–21:48	3600–4600	G, C	5
06-12-2006	09:07	V/T	SE	190–24	16–3		G, C	5
12/14-12-2006	01:00/14:00				Clouds		G, C; clouds	5
12-12-2006	21:09	T	NW	65–2		3300–3600	G, C	5

References

Allard, P., Carbonelle, J., Dajlevic, D., Le Bronec, J., Morel, P., Robe, M.C., Maurenas, J.M., Pierret, R.F., Martins, D., Sabroux, J.C., Zettwoog, P., 1991. Eruptive and diffuse emission of CO_2 from Mount Etna. Nature 351, 387–389.

Alparone, S., Andronico, D., Lodato, L., Sgroi, T., 2003. Relationship between tremor and volcanic activity during the Southeast Crater eruption on Mount Etna in early 2000. J. Geophys. Res. 108 (B5), 2241. doi:10.1029/2002JB001866.

Alparone, S., Andronico, D., Sgroi, T., Ferrari, F., Lodato, L., Reitano, D., 2007. Alert system to mitigate tephra fallout hazards at Mt. Etna Volcano, Italy. Nat. Hazards 43, 333–350.

Andò, B., Pecora, E., 2006. An advanced video-based system for monitoring active volcanoes. Comput. Geosci. 32 (1), 85–91.

Andronico, D., Scollo, S., 2006. Attività esplosiva al Cratere di SE - 8 novembre. Internal report at http://www.ct.ingv.it/Report/WKRVGCEN20061108.pdf.

Andronico, D., Cristaldi, A., Del Carlo, P., Taddeucci, J., 2003. Monitoring the ashes from the 2002–2003 flank eruption of Mount Etna (Italy). EAE03-A-06783, EGS-AGU-EUG Joint Assembly abstract.

Andronico, D., Branca, S., Calvari, S., Burton, M.R., Caltabiano, T., Corsaro, R.A., Del Carlo, P., Garfì, G., Lodato, L., Miraglia, L., Murè, F., Neri, M., Pecora, E., Pompilio, M., Salerno, G., Spampinato, L., 2005. A multi-disciplinary study of the 2002–03 Etna eruption: insights for a complex plumbing system. Bull. Volcanol. 67, 314–330.

Andronico, D., Cristaldi, A., Lo Castro, D., Scollo, S., Taddeucci, J., 2007a. The 24 November 2006 paroxysm at south-east crater, Mt. Etna. Proceedings of the XXIV General Assembly of the IUGG, Perugia July 2–13, 2007.

Andronico, D., Spinetti, C., Cristaldi, A., Buongiorno, M.F., 2007b. Mt. Etna ash plume during 2006 eruptions: integrated approach from satellite remote sensing and ground-based monitoring system. EGU2007-A-09585 Session GMPV7, EGU Conference abstract.

Andronico, D., Scollo, S., Cristaldi, A., Caruso, S., 2008. The 2002–03 Etna explosive activity: tephra dispersal and features of the deposit. J. Geophys. Res. 113 (B04209). doi:10.1029/2007JB005126.

Andronico, D., Scollo, S., Cristaldi, A., Ferrari, F., 2009. Monitoring the ash emission episodes at Mt. Etna: the 16 November 2006 case study. J. Volcanol. Geotherm. Res. 180, 123–134 (this issue). doi:10.1016/j.jvolgeores.2008.10.019.

Branca, S., Consoli, S., 2006. Rapporto eruzione Etna (15 Luglio 2006, aggiornamento ore 05:00 locali). Internal report at http://www.ct.ingv.it/Report/WKRVG20060715.pdf.

Branca, S., Polacci, M., 2006. Aggiornamento attività eruttiva dell'Etna (04 Ottobre 2006, ore 14:00 locali). Internal report at http://www.ct.ingv.it/Report/WKRVGREP20061004_1400.pdf.

Bruno, N., Caltabiano, T., Giammanco, S., Romano, R., 2001. Degassing of SO_2 and CO_2 at Mount Etna (Sicily) as indicator of pre-eruptive ascent and shallow emplacement of magma. J. Volcanol. Geotherm. Res. 110, 137–153.

Volcanic ash and aviation safety. In: Casadevall, T.J. (Ed.), Proceedings of the First International Symposium on Volcanic Ash and Aviation Safety. U.S. Geological Survey Bulletin, vol. 2047, p. 450.

Calvari, S., 2006a. Comunicato Etna del 26 ottobre 2006 aggiornamento alle ore 10:00. Internal report at http://www.ct.ingv.it/Report/20061026-1000.pdf.

Calvari, S., 2006b. Aggiornamento attività Etna (16 novembre 2006, ore 10:30 locali). Internal report at http://www.ct.ingv.it/Report/20061116-1030web.pdf.

Calvari, S., Lodato, L., 2006. Aggiornamento dell'attività eruttiva dell'Etna al 5 settembre 2006 - ore 9:30. Internal report n° UFVG2006/103 at http://www.ct.ingv.it/Report/20060905-0930.pdf.
Coltelli, M., 2006. Aggiornamento attività Etna (28 ottobre 2006, ore 17:00 locali). Internal report at http://www.ct.ingv.it/Report/WKRVG20061028-1.pdf.
Cristaldi, A., Scollo, S., 2006. Rapporto sull'emissione di cenere all'Etna nei giorni 29 e 31 ottobre 2006. Internal report n. UFVG2006/128 at http://www.ct.ingv.it/Report/rptvgcenere20061102.pdf.
FAA (U.S.A.) Aviation Weather Directorate, 2001. User Needs Analysis Document: Volcanic Activity. Version 1.0, 5 Sept 2001.
Filizzola, C., Lacava, T., Marchese, F., Pergola, N., Scaffidi, I., Tramutoli, V., 2007. Assessing RAT (Robust AVHRR Techniques) performances for volcanic ash cloud detection and monitoring in near real-time: the 2002 eruption of Mt. Etna (Italy). Rem. Sens. Environ. 107, 440–454.
Francis, P., Rothery, D., 2000. Remote Sensing of active volcanoes. Annu. Rev. Earth Planet. Sci. 28, 81–106. doi:10.1146/annurev.earth.28.1.81.
Gary, D., 2007. History of the NOAA satellite program. J. Appl. Rem. Sens. 1, (012504).
Hufford, G.L., Salinas, L.J., Simpson, J.J., Barske, E.G., Pieri, D.C., 2000. Operational implications or airborne volcanic ash. Bull. Amer. Meteor. Soc. 81 (4), 745–755.
Haulet, R., Zettwoog, P., Sabroux, P.C., 1977. Sulphur dioxide discharge from Mount Etna. Nature. 268, 715–717.
Holasek, R.E., Self, S., Woods, A.W., 1996. Satellite observations and interpretation of the 1991 Mount Pinatubo eruption plumes. J. Geophys. Res. 101, 27635–27665.
ICAO, 2004. International civil aviation organisation international handbook on the International Airways Volcano Watch (IAVW)—operational procedures and contact list, ICAO Document 9766-AN/968, Second ed.
INGV-STAFF, Sezione di Catania, 2001. Multidisciplinary approach yields insight into Mt. Etna 2001 eruption. EOS Trans. AGU 82 (52), 653–656.
Matsushima, N., Shinohara, H., 2006. Visible and invisible plumes. Geophys. Res. Lett. 33, L24309. doi:10.1029/2006GL026506.
Miller, T.P., Casadevall, T.J., 2000. Volcanic ash hazards to aviation. In: Sigurdsson, H. (Ed.), Encyclopedia of Volcanoes. Academic Press, San Diego, California, USA, pp. 915–930.
NOAA, 2000. NOAA KLM User's Guide. Available at http://www2.ncdc.noaa.gov/docs/intro.htm.
Norini, G., De Beni, E., Andronico, D., Polacci, M., Burton, M., Zucca, F., 2008. The 16 November 2006 flank collapse of South-East Crater at Mount Etna, Italy: study of the deposit and hazard assessment. J. Geophys. Res., in revision.
Pergola, N., Tramutoli, V., Marchese, F., Scaffidi, I., Lacava, T., 2004. Improving volcanic ash cloud detection by a robust satellite technique. Rem. Sens. Environ. 90, 1–22.
Pieri, D., Ma, C., Simpson, J.J., Hufford, G., Grindle, T., Grove, C., 2002. Analyses of in-situ airborne volcanic ash from the February 2000 eruption of Hekla Volcano, Iceland. Geophys. Res. Lett. 29, 19–1–19-4.
Prata, A.J., 1989a. Observations of volcanic ash clouds in the 10–12 μm window using AVHRR/2 data. Int. J. Rem. Sens. 10 (4–5), 751–761.
Prata, A.J., 1989b. Infrared Radiative transfer calculations for volcanic ash clouds. Geophys. Res. Lett. 16 (11), 1293–1296.
Prata, A.J., Grant, I.F., 2001. Determination of mass loadings and plume 1 heights of volcanic ash clouds from satellite data. CSIRO Atmosph. Res. Tech. Pap. 48, Commonw. Sci. and Ind. res. Organ., Melbourne, Victoria, Australia, p. 39.
Prata, A.J., Bluth, G.J.S., Rose, W.I., Schneider, D.J., Tupper, A.C., 2001. Comments on "Failures in detecting volcanic ash from a satellite-based technique. Rem. Sens. Environ. 78, 341–346.
Schneider, D.J., Rose, W.I., Kelley, L., 1995. Tracking of 1992 eruption clouds from Crater Peak of Mount Spurr Volcano, Alaska, using AVHRR. U. S. Geol. Surv. Bull. (Spurr Eruption, edited by T. Keith), vol. 2139, pp. 27–36.
Scollo, S., Del Carlo, P., Coltelli, M., 2007. Tephra fallout of 2001 Etna flank eruption: Analysis of the deposit and plume dispersion. J. Volcanol. Geotherm. Res. 160, 147–164.
Self, S., Holasek, R.E., 1995. GOES weather satellite observations and measurements of the May 18, 1980, Mount St. Helens eruption. J. Geophys Res. 100 (B5), 8469–8488.
Simpson, J.J., Hufford, G., Pieri, D., Berg, J.S., 2000. Failures in detecting volcanic ash from a satellite-based technique. Remote Sens. Environ. 72, 191–217.
Simpson, J.J., Hufford, G., Pieri, D., Berg, J.S., 2001. Response to "Comments of Failures in detecting volcanic ash from a satellite-based technique. Remote Sens. Environ. 78, 347–357.
Simpson, J.J., Hufford, G., Pieri, D., Servranckx, R., Berg, J., Bauer, C., 2002. The February 2001 eruption of Mount Cleveland, Alaska: case study of an aviation hazard. Weather Forecast 17, 691–704.
Sparks, R.S.J., Bursik, M., Carey, S., Gilbert, J., Glaze, L., Sigurdsson, H., Woods, A.W., 1997. Volcanic Plume. John Wiley & Sons, Inc., Chichester, England, p. 574.
Spinetti, C., Buongiorno, M.F., Lombardo, V., Merucci, L., 2003. Retrieval aerosol optical thickness of volcanic plumes by means of the airborne Multispectral Image Spectrometer (MIVIS): a case study from Mt. Etna Sicily, June 1997. Ann. Geophys. 6 (2), 439–449.
Spinetti, C., Buongiorno, M.F., 2007. Volcanic Aerosol optical characteristics of Mt. Etna tropospheric plume retrieved by means of airborne multispectral images. J. Atm. Sol. Ter. Phys. 69 (9), 981–994. doi:10.1016/j.jastp.2007.03.014.
Spinetti, C., Andronico, D., Taddeucci, J., Cristaldi, A., Buongiorno, M.F., 2007. Ash plumes at MT. Etna during the 2006 eruption: observations from satellite to microscope. Paper presented at the IUGG Conference, Session VS015.
Spinetti, C., Corradini, S., Merucci, L., Silvestri, M., Musacchio, M., Buongiorno, M.F., 2008. Volcanic ash plume at Mt. Etna using polar and geostationary satellite data: the 24 November 2006 eruption event. Paper presented at the IAVCEI Conference, Session VS015.
Tupper, A., Kinoshita, K., Kanagaki, C., Iino, N., Kamada, Y., 2003. Observations of volcanic cloud heights and ash–atmosphere interactions. Proc of WMO/ICAO Third International Workshop on Volcanic Ash, Toulouse, France, September 29–October 3, 2003.
Tupper, A., Carn, S., Davey, J., Kamada, Y., Potts, R., Prata, F., 2004. An evaluation of volcanic cloud detection techniques during recent significant eruption in the western 'Ring of Fire'. Remote Sens. Environ. 91, 27–46.
Tupper, A., Davey, J., Stewart, P., Stunder, B., Servranckx, R., Prata, F., 2006. Aircraft encounters with volcanic clouds over Micronesia, Oceania, 2002–03. Aust. Meteorol. Mag. 55, 289–299.
Young, T.L., 2006. TeraScan 0.46 m/0.61m/1.2m/1.5m Polar Satellite Tracking Antenna O&M Manual. Seaspace, January 2006.
Yu, T., Rose, W., Prata, A.J., 2002. Atmospheric correction for satellite-based volcanic ash mapping and retrievals using "split window" IR data from GOES and AVHRR. J. Geophys Res. 107 (16). doi:10.1029/2001JD000706.
Wen, S., Rose, W.I., 1994. Retrieval of sizes and total masses of particles in volcanic clouds using AVHRR bands 4 and 5. J. Geophys. Res. 99 (D3), 5421–5431.